HHS Public Access

Author manuscript

J Neurogenet. Author manuscript; available in PMC 2016 July 14.

Published in final edited form as:

J Neurogenet. 2015 ; 29(0): 135–143. doi:10.3109/01677063.2015.1064916.

Drosophila mutants of the autism candidate gene *neurobeachin* (*rugose*) exhibit neuro-developmental disorders, aberrant synaptic properties, altered locomotion, impaired adult social behavior and activity patterns

Alexandra Wise[1], **Luis Tenezaca**[1], **Robert W. Fernandez**[2], **Emma Schatoff**[1], **Julian Flores**[1], **Atsushi Ueda**[3], **Xiaotian Zhong**[3], **Chun-Fang Wu**[3], **Anne F. Simon**[4,*], and **Tadmiri Venkatesh**[1,*]

[1]Department of Biology, City College of New York, NY 10031

[2]Department of Molecular Biophysics and Biochemistry, Yale University

[3]Department of Biology, University of Iowa, Iowa City, IA 52242

[4]Department of Biology, Western University, Ontario, Canada

Abstract

Autism spectrum disorder (ASD) is a neurodevelopmental disorder in humans characterized by complex behavioral deficits, including intellectual disability, impaired social interactions and hyperactivity. ASD exhibits a strong genetic component with underlying multi-gene interactions. Candidate gene studies have shown that the *neurobeachin* gene is disrupted in human patients with idiopathic autism (Castermans et al., 2003). The gene for *neurobeachin* (*NBEA*) spans the common fragile site FRA 13A and encodes a signal scaffold protein (Savelyeva et al., 2006). In mice, *NBEA* has been shown to be involved in the trafficking and function of a specific subset of synaptic vesicles. (Medrihan et al., 2009; Savelyeva, Sagulenko, Schmitt, & Schwab, 2006). *rugose (rg)* is the *Drosophila* homologue of the mammalian and human *neurobeachin*. Our previous genetic and molecular analyses have shown that *rg* encodes an A kinase anchor protein (DAKAP 550), which interacts with components of the EGFR and Notch mediated signaling pathways, facilitating cross-talk between these and other pathways (Shamloula et al., 2002). We now present functional data from studies on the larval neuromuscular junction that reveal abnormal synaptic architecture and physiology. In addition, adult *rg* loss-of-function mutants exhibit defective social interactions, impaired habituation, aberrant locomotion and hyperactivity. These results demonstrate that *Drosophila neurobeachin* (*rugose*) mutants exhibit phenotypic characteristics reminiscent of human ASD and thus could serve as a genetic model for studying autism spectrum disorders.

*Authors for correspondence: Tadmiri Venkatesh, Department of Biology, City College of New York, New York, NY 10031, Tel: 212-650-8469, Fax: 212-650-8585, venky@sci.ccny.cuny.edu. Anne F. Simon, Biology Department, Western University, London, Ontario, Canada, N6A 3K7, Tel: 519-661-2111 X 80084, Fax: 519-661-3935, asimon28@uwo.ca.

Keywords

Drosophila; rugose; neurobeachin; Autism Spectrum Disorder; synaptic development; neuromuscular junction

INTRODUCTION

Autism spectrum disorder (ASD) is a debilitating human neurodevelopmental disorder exhibiting a complex array of symptoms such as learning deficits, hyperactivity, anxiety, impaired social behavior and cognition (Geschwind, 2009). ASDs are currently estimated to occur at a frequency of 1% in the general population making them one of the most common neurodevelopmental disorders (Kim et al., 2011). Recent studies have demonstrated a strong genetic component with underlying genetic interactions modulating ASD characteristics. The ASD characteristics and the related phenotypes are vastly heterogeneous among individuals and frequently show incomplete penetrance. Genetic studies involving a variety of approaches including copy number variation, single gene mutations, SNP analyses, whole genome linkage and gene association studies have implicated several hundred genes in ASD and current estimates suggest that genetic factors account for about 10–20% of the reported ASD cases (Abrahams & Geschwind, 2008; Banerjee, et al., 2014). In addition, a vast amount of data suggest that environmental and epigenetic factors contribute significantly to the etiology of the ASD phenotypes and are recognized as modulating factors (Banerjee et al., 2014). Nevertheless, the precise etiology and dependable risk factors for ASD are elusive. Mutational studies in animal model systems have implicated several conserved proteins regulating synaptic structure and function in ASD-like phenotypes. In several cases, human ASD patients have been shown to carry disruptions in the genes encoding these synaptic proteins (Banerjee et al., 2014), giving rise to the possibility that such proteins could serve as therapeutic targets.

Recent human genetic studies have identified *neurobeachin* (*NBEA*) as a candidate gene for ASD following initial reports that a chromosomal translocation with a breakpoint within the *NBEA* gene resulted in idiopathic autism in adolescent males (Castermans et al., 2003). This work was followed by additional reports of ASD patients with deletions in the *NBEA* gene (O'Neal et al., 2009; Volders et al., 2011). The *neurobeachin* gene spans the common fragile site *FRA 13A* (Savelyeva et al., 2006) and encodes a large multi-domain scaffolding protein initially identified as a protein Kinase A anchoring protein (AKAP). Studies in animal model systems have shown that NBEA is involved in a variety of cellular processes such as retinal patterning (Shamloula et al., 2002), membrane vesicular trafficking and neurotransmitter release (Castermans et al., 2003; Nair et al., 2013), short term memory consolidation (Volders et al., 2012; Zhao et al., 2013), and platelet development and function (Nuytens et al., 2013). In this paper, we present data, which show that *rugose*, the *Drosophila neurobeachin* (*DNBEA*) loss-of-function mutants exhibit aberrant larval locomotion and abnormal synaptic architecture and physiology. Adult *NBEA* mutants show impaired habituation, hyperactivity and altered social behavior. These results demonstrate that *Drosophila neurobeachin (rugose*) mutants exhibit phenotypic characteristics

reminiscent of human ASD and thus could serve as a genetic model for studying Autism spectrum disorders.

METHODS

Drosophila Culture

Flies were maintained on standard cornmeal–agar medium and kept at 23° C. The *rugose* (*rg)* mutant alleles used in this study have been described previously (Shamloula et al., 2002) and they include the alleles $rg^{\gamma 1}$, $rg^{\gamma 5}$, $rg^{\gamma 7}$, $rg^{\gamma 8}$, $rg^{\gamma 9}$, $rg^{\gamma 11}$ *and* rg^{p2}, rg^{p4}, rg^{p5}*and* rg^{p6}. We compared these lines to the original *Canton-S* (CS) stock that was used to generate the mutant alleles.

Immunocytochemistry

Males from third-instar larvae were selected and dissected in modified hemolymph-like solution HL3.1(Feng et al., 2004) and fixed for 25 min in 4% paraformaldehyde. The preparations were washed three times for 5 minutes with 0.2 M Phosphate Buffer Solution containing 0.2% Triton-X 100 (PBST). The whole mount preparations of dissected larvae were incubated overnight at 4°C in mouse anti-Discs Large (anti-Dlg) monoclonal antibody (mAb, supernatant 4F3, University of Iowa Developmental Studies Hybridoma Bank) at a dilution of 1:5. The preparation were then washed 3 times (5 minutes each time) in 0.2 % PBST. Secondary antibodies were applied for 2 hours: Alexa Fluor 635 conjugated anti-Phalloidin at dilution of 1:1000 (Invitrogen); FITC-conjugated goat anti-mouse (Jackson Laboratories) diluted1:100 and TRITC-conjugated goat anti-Horseradish Perioxidase (Jackson Laboratories) at a dilution of 1:100. Preparations then were washed twice for 5 min and mounted using Vectashield (Vector Laboratories). Confocal microscope images were taken with LSM 510 Confocal Laser Scanning System (Carl Zeiss Inc.) and processed with Image J 1.24 and Adobe Photoshop 5.5. Type 1b boutons were counted using muscles 6 and 7 from segments A2 and A3 and analyzed using GraphPad Prism. Counts were analyzed by ACT-1 software (Nikon Digital Eclipse DXM 1200) and p values were determined by Student's two-tailed t-test (Prism).

Larval EJP recording

We dissected post-feeding third instar larvae and recorded excitatory junctional potentials (EJPs) from muscles # 6 and 7 of abdominal segments 3 and 6, as described previously (Jan et al., 1977; Wu et al., 1978). Briefly, larvae were dissected in Ca^{2+} free HL3 saline (Stewart et al., 1994) containing 70mM NaCl, 5mM KCl, 20mM $MgCl_2$, 10mM $NaHCO_3$, 5mM Trehalose, 115mM Sucrose, and 5mM HEPES, at pH 7.2. EJPs were recorded in low Ca^{2+} HL3.1 (Feng et al., 2004), which has the same ionic composition except for a reduced Mg^{2+} concentration (4mM). The final Ca^{2+} concentration in recording saline is specified for each experiment. To evoke EJPs, the segmental nerves were severed from the ventral ganglion and stimulated with a suction electrode (10μm inner diameter) through the cut end. Stimulation amplitude was adjusted to 2.0 times the threshold voltage to ensure a uniform stimulation condition among experiments. Stimulus duration was 0.1 ms. Intracellular glass microelectrodes were filled with 3 M KCl and had a series resistance of about 60 MΩ. EJPs

were recorded with direct current pre-amplifiers (model M701 micro-probe system, WPI, Conn., USA) and an additional custom-built amplifier.

Adult Habituation

Preparation of flies, stimulation, recording, and analysis of muscle responses were performed as described previously (Engel & Wu, 1992, 1996) with some modifications. The Faraday cage was covered with black plastic to reduce ambient light because strong illumination was found to inhibit the long-latency response. Stimulation (0.1 ms pulse, Grass S8, Quincy MA) was passed between insulated tungsten electrodes inserted in the eyes. Signals were recorded from the right tergotrochanteral (TTM) jump muscle and left dorsal longitudinal a (DLMa) flight muscle, which are innervated by the same side of the giant fiber pathway (Levin et al., 1992; Thomas & Wyman, 1984). Muscle response probability and the number of stimuli to failure criterion were analyzed as described previously (Engel & Wu, 1996, 1998).

Behavior assays

Larval Peristaltic Contraction Counting Assay Protocol—Agar plates were made using 12.5% ultra-pure agarose and stored at 4°C and were incubated at 30°C for 15 min before use as previously described (Nagai, Hashimoto, & Yamaguchi, 2010). A 12 well plate was used for washing the larvae, 6 wells were filled with 500uL deionized (d.i.) water, and 6 with 500 uL 15% sucrose solution. Late third instar larvae in the wandering stage were identified as crawling on the side of the bottle (not submerged in the food). They were removed from the bottle using a paintbrush, and about 3–5 larvae were placed in each of the sucrose wells. The well plate was placed on a shaker for 1 wash (7 minutes). The larvae were then transferred from the sucrose wells to the d.i. water wells with a paintbrush, and returned to the shaker for 2 washes (14 minutes). An individual larva was then removed from a well, placed on the agar plate, and allowed to acclimate for 30 seconds. The number of peristaltic contractions was counted for 2 minutes. If the larva was still alive at the end of 2 minutes but no contractions had been observed, it was discarded and the trial was redone with a different larva. 100 larvae were observed for each mutant strain.

Larval Locomotion Analysis—Further locomotion studies were performed on third instar “wandering” larvae using Multi-Worm Tracker software (Janelia Farm). MWT software tracks, in real time, small, moving high-contrast objects against a static background. Larvae were first washed in dH_2O and then placed on thinly coated 1.5% agar gel plates that were imaged with a Nikon camera. Each trial contained approximately five larvae and total of 15 trials were used for each *rg* mutant allele. Up to five larvae at a time were allowed to remain on the plate for 62 seconds while the software captured their images. After 62 seconds, the larvae were discarded and five new larvae were plated on the same agar plate. Data on speed, length, angular speed and kink were collected and compiled in Excel and analyzed in GraphPad Prism 5. Speed refers to the speed of the centroid in mm/second, that is, how fast each larva crawled. Angular speed was measured in radians/second of objects; this is calculated over the same interval as speed, but reports the greatest difference in angle between primary axes over that time. Length refers to the distance spanned by objects along their major axis (defined to be the axis of a least squares fit), in

mm. Kink, was defined by the angle in radians between the line from the first to third point of the skeleton and the fourth through last points. Mean length refers to the average length of the larvae in pixels. Current length refers to length in pixels at any given time. Average relative length of object is derived from relative length which is, current length / mean length (MWT User Manual, Janelia Farm).

Fly Handling in Adult Social Behavior assays

Fly husbandry was conducted in a 23°C incubator, and the behaviors assays were performed at room temperature (22–25°C). Flies were reared in bottles, and males were collected at 3–7 days old, under cold anesthesia, placed 40 per vial, to recover overnight. The flies were allowed to habituate for two hours in vials with fresh food in the room in which the test was performed. All experiments were run at least three independent times with two to three internal replicates of 40 flies each.

Avoidance of Drosophila Stress Odorant (dSO)

Assays for the avoidance of social stress odorant were conducted using a T-maze with an n=40 tester male fly group, and around 70 mixed gender CS emitters flies, as described in Suh et al. (2004) and Fernandez et al. (2014). Emitter flies were agitated on a vortex mixer in 15 sec. bouts, at 5 sec. intervals, over a 1-min period, and then discarded. The empty tube was placed on one side of the choice point of the T-maze, facing a fresh tube. Tester flies were placed in the T-maze's elevator to habituate for 1 minute, after which they were placed at the choice point and allowed to choose between the dSO containing tube and the fresh tube for 1 minute. The Performance Index (PI) was calculated as the percentage of flies able to avoid the dSO by moving to the fresh tube minus those that moved into the dSO containing tube or stayed in the middle of the maze. A PI of zero indicates a 50–50 distribution: no avoidance; a PI of 100 indicates that all the flies avoided the dSO.

Social Space Assays

Social space assays were conducted using vertical triangle chambers with 40 flies. Pictures were taken once the flies reached a stable clustering, in which limited or no motion is seen, as described (Simon et al., 2012; Fernandez et al., 2014). Because the mutant flies were hyperactive, such stable clustering was not reached until 40 minutes after flies were placed in chambers. This time delay does not affect social space in CS flies (Simon et al., 2012). Digital images were imported in ImageJ software (NIH, rsbweb.nih.gov/ij) and analyzed for nearest neighbor distances as described in (Burg et al., 2013). These data were imported into GraphPad Prism 6 for further analysis. Instead of using the previously reported Social Space Index, which is an indirect representation of the data (Burg et al., 2013; Simon et al., 2012), we choose here to directly represent the distribution of the distances using boxes and Tukey's whiskers plots, as a statistical tool to eliminate outliers. Because the distribution of the distance was non-Gaussian, statistical analyses were performed using Kruskal-Wallis tests and Dunn's multiple comparisons post-tests.

Drosophila Activity Assay

To conduct the adult locomotor assay, groups of 1–3 day old male flies from each strain were maintained in sealed tubes and were placed in *Drosophila* activity monitors (Trikinetics) housed inside a humidified incubator (Digitherm), where temperature (25° C) and humidity level were kept constant. Prior to recording, the flies were given a day to acclimatize to their new environment. Flies'average activity was then recorded in thirty-minute bins throughout four days under a 12:12 hour light: dark cycle. The activity recorded for each bin was determined by how many times each individual fly crossed an infrared light beam that bisected the capillary tube and was perpendicular to the tube. Results for each strain are expressed as the mean daily activity bouts over a four-day interval.

RESULTS

rg mutants show changes in synaptic bouton number and morphology

All of the *rugose* mutant alleles tested ($rg^{\gamma 1}$, $rg^{\gamma 4}$, $rg^{\gamma 5}$, $rg^{\gamma 6}$, $rg^{\gamma 7}$,, $rg^{\gamma 8}$, $rg^{\gamma 9}$, $rg^{\gamma 11}$ rg^{P2}, rg^{P3}, rg^{P4}, rg^{p5} *and* rg^{P6}) showed abnormal type 1 bouton morphology (Figure 1) when compared to the wild type (CS) strain. Boutons in the mutants were less oval shaped and more oblong compared to those in the wild type. In addition, the boutons had grown continuously and connected with each other, forming a single large bouton. By comparison, CS boutons were more discretely oval-shaped. *rg* mutant boutons also appeared to be enlarged and some boutons, specifically in mutant alleles $rg^{\gamma 8}$ and $rg^{\gamma 9}$ contained spaces that had no staining, appearing as vacuolated blebs (arrow, Figure 1). To assess whether bouton sizes were altered in *rg* mutants, we used Image J software to measure and analyze bouton sizes in several *rg* mutants. Our results showed that *rg* mutant bouton sizes were not significantly different when compared to CS (data not shown). There were occasional outliers, which appeared to show an enlarged bouton. Compared to wild type, all the *rg* mutants examined showed significant decrease in the number of type 1 boutons except rg^{P2} which showed little or no change (Figure 2). Anti-Horseradish peroxidase (HRP) positive staining was used for bouton counts performed on muscles 6 and 7 in segment A2. Type-II boutons positive for anti-HRP but not anti-Dlg also had significant decrease in bouton number (data not shown).

Evoked responses and Short-term plasticity are altered in *rugose* mutants

In order to examine the role of Rugose in synaptic function at the cellular level, we examined the properties of neuromuscular transmission in third-instar larvae. This preparation has been used extensively for studies on synaptic function (Jan et al., 1977; Wu et al., 1978), development (Broadie & Bate, 1993; Keshishian & Kim, 2004; Kidokoro & Nishikawa, 1994), plasticity (Budnik et al., 1990; Zhong & Wu, 1991a, 1991b; Sigrist et al., 2003; Ueda & Wu, 2009), and transmitter vesicle mechanisms (Kuromi et al., 2010; Ramaswami et al., 1994; Song et al., 2002). It is therefore ideal for characterizing physiological properties in *rg* mutants. We found that in saline containing low Ca^{2+} (0.2 mM), nerve-evoked EJPs in *rg* mutants ($rg^{\gamma 1}$ *and* $rg^{\gamma 7}$) were abnormally large compared to those in wild type controls (Figure 3A and B). This reflects increased transmitter release, because the sizes of spontaneous miniature EJPs were similar between *rg* and wild type larvae (*rg*, 1.9 ± 0.68 mV, n = 4; WT, 1.5 ± 0.48 mV, n = 7, $p > 0.05$). In addition, the short-

term plasticity was altered, as evidenced by abnormal response to paired-pulse stimulation. We observed a weakened paired-pulse facilitation in *rg* mutants at the same Ca^{2+} level (Figure 3C), likely correlated to the greater transmitter release from *rg* presynaptic terminals. At a 100-ms inter-pulse interval, wild type showed clear facilitation, while *rg* showed no clear facilitation. At a shortened inter-pulse interval, 50 ms, the facilitation of EJP amplitude was masked by the non-linear summation to the first response.

Larval locomotion is abnormal in *rugose* mutants

To test, whether *rugose* mutants show impairments in locomotion due to previously described changes in synaptic physiology, we conducted locomotion assays. We observed significant locomotory deficiencies in all of the mutant alleles tested. In one assay, the number of peristaltic contractions of wandering third-instar larvae was recorded in severe *rg* mutants: $rg^{\gamma 1}$, $rg^{\gamma 5}$, $rg^{\gamma 7}$ and in wild type. Peristaltic contractions alternate between shortening and lengthening phases in a rhythmic motion that allow the larva to move. These peristaltic waves are generated by a central pattern generator and can be easily observed by the naked eye (Choi et al., 2004). Although the larvae generally wandered in random directions, wild-type larvae on average contracted more frequently than any of the mutant strains (Figure 4A). Peristaltic behavior was most severely impaired in $rg^{\gamma 7}$ (n= 100, $p<0.0001$), followed by $rg^{\gamma 5}$ (n= 100, $p<0.0001$), and $rg^{\gamma 1}$ (n=100, $p<0.0001$) (Figure 4C). To determine whether the altered the peristaltic movements in *rg* mutants changed the overall characteristics of locomotion, such as speed and kink, we used the Worm tracker (MWT) software. The average speed of the larvae was significantly slower in $rg^{\gamma 1}$ (n= 102, $p<0.0001$), $rg^{\gamma 4}$ (n=100, $p<0.0001$), $rg^{\gamma 5}$ (n=103, $p<0.0001$), $rg^{\gamma 7}$ (n=100, $p<0.0001$), $rg^{\gamma 9}$ (n=103, $p<0.0001$), and $rg^{\gamma 11}$ (n=102, $p<0.0001$) compared to wild type (Figure 4B). Kink was significantly elevated in mutants, $rg^{\gamma 1}$ (n= 102, $p<0.0001$), $rg^{\gamma 4}$ (n=100, $p<0.0001$), $rg^{\gamma 5}$ (n=103, $p<0.0001$), $rg^{\gamma 7}$ (n=100, $p<0.0001$), $rg^{\gamma 9}$ (n=103, $p<0.0001$) and $rg^{\gamma 11}$ (n=102, $p<0.0001$) (Figure 4C). This elevation in kink indicates that mutant *rg* larvae were more likely to be in a curled position and less likely to be linear. However, larval length was not significantly changed (Figure 4D). As a result, mutant larvae moved more slowly than control larvae and were more often in the curled posture.

Adult *rugose* mutants show altered habituation

To investigate how adult behavior was affected by the *rugose* mutations, we tested habituation, locomotion and activity levels, and response to social signals. Habituation is a form of non-associative plasticity in which there is a reduction in response to a specific stimulus presented repetitively over time. Flight muscles are driven by a central pattern generator for flight, but are also associated with the adult giant fiber escape response (Engel & Wu, 1996) which can be used in habituation studies. In adult flies, changes in synaptic properties are evident in *rg* mutants. Indeed, $rg^{\gamma 5}$, $rg^{\gamma 6}$ and $rg^{\gamma 7}$ mutants showed strong increase in the rate of habituation, that is, it takes a significantly shorter time interval for the giant fiber circuit to habituate in the *rg* mutant alleles than wild type, with $rg^{\gamma 7}$ being the most severe, followed by $rg^{\gamma 6}$ and $rg^{\gamma 5}$ (Figure 5A). This was clear when determined with a criterion of the number of stimuli necessary to reach 5 consecutive failures in response to 5-Hz stimulus train. The number of stimuli to different failure criteria (1, 2, 5, 20) is significantly decreased in the mutants $rg^{\gamma 5}$, $rg^{\gamma 6}$, and $rg^{\gamma 7}$, i.e., the number of stimuli to

attain a number of consecutive failures was decreased in *rugose* mutants compared to wild type. The differences between habituation rates in *rg* and wild type became even more striking if a criterion of 20 consecutive failures was applied (Figure 5B). Plotting the mean number of stimuli to attain criteria of one to twenty consecutive failures (Figure 5B) shows that more rapid habituation occurs consistently among *rg* mutants, regardless of the criterion number.

Adult *rugose* mutants exhibit hyperactivity

rg mutants tend to be visibly hyperactive (see also social space below). To quantify whether they had an increase in movement over time, in the absence of any stimuli, we used a Trikinetic Drosophila activity monitor. All mutants tested displayed about 200 to 400% increase in activity bouts compared to wild type (Figure 6).

Decreased avoidance to the stress odorant (dSO)

CS flies strongly avoid the dSO left by agitated flies (Figure 7A) as shown previously (Suh et al., 2004; Fernandez et al. 2014). In contrast, both rg^{p2} and rg^{p6} mutants displayed a decreased performance compared to CS. Although the mean PI is reduced only by 23% and by 30% respectively for rg^{p2} and rg^{p6} compared to CS (Figure. 7A), these results indicate that they were not as efficient in avoiding the stress odor left by agitated flies. There was a wider range of performances in mutants on this test, an internal variation reflected by the larger SEM in mutants as compared to CS.

Increased social space with, closest neighbor in *rugose* mutants

As previously described, 50% of the CS flies stayed closer than 0.25 cm, or slightly more than one-body length (Fig. 7B and Simon et al., 2012). The distribution of both rg^{p2} and rg^{p6} mutants was much more variable, with the flies staying further apart: 50% settled more than 0.38 cm for rg^{p6} and 0.47 cm for rg^{p2} apart from each other, more than two body lengths apart (Figure. 7B). The mutant flies also displayed a more variable preferred distance, with a larger range. In fact, their distribution within the chamber is not different from that of flies with no social interactions, as measured by testing single flies 40 times, and merging the data into a single combined image, as performed in (Simon et al., 2012 and Fig. 7B). This comparison also serves as a control for the effect of hyperactivity, centrophobism and geotaxis. That is *rg* mutants behave as if there were no other flies in the chamber.

DISCUSSION

Data presented here implicate *Drosophila* Rugose in synaptic development, physiology and adult behavior. Our studies on the larval NMJ showed altered morphological features and physiological properties of the synapses. *rg* mutants showed significant decreases in the number of boutons at the NMJ, altered bouton shapes and no significant changes in the bouton size. Overall, there was a decrease in the number of boutons in all of the alleles tested. Our electrophysiological studies on the larval neuromuscular junction showed an increase in the size of individual EJPs, and synapses also showed pair-pulse depression compared to facilitation in the CS control with repetitive stimuli. In addition, our data show

that *rg* mutant larvae display aberrant locomotor behavior with decreases in peristaltic movement and speed, and alterations in posture. These findings are consistent with a functional role for Rugose at the synapse.

Rugose is the *Drosophila* homolog of the mammalian Neurobeachin (NBEA), a scaffolding protein implicated in neurotransmitter /endomembrane vesicle trafficking at the synapse. Other studies on NBEA lend further support to its functional role at the synapse. In mice, loss-of-function of NBEA protein completely blocks evoked synaptic transmission at neuromuscular junctions while nerve conduction, synaptic structure and spontaneous neurotransmitter release remain normal. NBEA has also been implicated in vesicular traffic at the synapse and has been shown to be required for normal development of the synapses (Medrihan et al., 2009). Recent studies have shown that the *NBEA* gene is disrupted in individuals with Autism spectrum Disorder and the *NBEA* gene spans the common Fragile site FRA 13A in human (Savelyeva et al., 2006). Individuals with Fragile X Syndrome and autism, have reduced levels of cAMP (Berry-Kravis & Ciurlionis, 1998). This has been shown to lead to a decrease in evoked synaptic potential, dendritic architecture and actin “clumping” in areas near the postsynaptic membrane (Medrihan et al., 2009; Niesmann et al., 2011).

Our results are consistent with earlier studies on the effects of altered cAMP metabolism on synaptic plasticity in adult *Drosophila* (Engel & Wu, 1996) and neurotransmission at the larval NMJ (Zhong & Wu, 1991a, 1991b). The modulation of the cAMP signaling at the synapse by Rugose may be through its function as a signal scaffold for Protein Kinase A or A kinase anchoring protein (AKAP) (Han, Baker, & Rubin, 1997; Shamloula et al., 2002). Mammalian AKAPs have been shown to maintain postsynaptic scaffolds by simultaneously associating with other kinases and phosphatases. For example, AKAP79/150 has been shown to be targeted to dendritic spines by a binding motif in the N-terminus which complexes with phosphatidylinositol–4, 5-bisphosphate (PIP_2), F-actin, and actin-linked cadherin adhesion molecules (Michel & Scott, 2002). Rugose may work in a similar manner, which would allow for changes in the appearance of synaptic boutons. AKAPs are key mediators of cAMP as well as other signal transduction pathways. Presynaptically, AKAPs have been shown to regulate ion channel function, particularly that of Ca^{2+} channels, which are required for vesicle fusion (Rizo & Sudhof, 2002). PKA and AKAPs together can increase the efficiency of these channels by 3- to 10 fold, allowing for greater current to flow (Pelzer et al., 1990). The molecular mechanism that directly links *rg* function to evoked synaptic transmission remains unclear, However, AKAPs have also been shown to directly interact with adenylate cyclase in neurons thereby regulating the amount of cAMP that is produced in the cell (Dell’Acqua et al., 2006). This may provide a mechanism by which changes in presynaptic vesicular release lead to observed changes in transmission and plasticity.

In humans, disruption of the *NBEA* gene results in idiopathic autism and the autistic individuals typically display hyperactivity and have difficulty with social interactions. To look for similar adult behavior correlates in flies, in addition to examining *rg* effects in larvae, we studied the consequences of *rg* mutation on the behavior of adult flies. We found that *rg* mutants are similarly both more active and are socially avoidant. Our conclusion is

based on outcomes of *rg* mutants' behavior in assays of social signals. We first tested the ability of the flies to avoid the *Drosophila* stress odorant (dSO) left by agitated flies in the avoidance assay (Suh et al., 2004; Fernandez et al, 2014). We also tested the flies' response to others in social clustering, the measure of distances to their closest neighbor (their social space), in a stable undisturbed group (Burg et al., 2013; Simon et al., 2012). Social space and social avoidance probably result from equilibrium between multiple attractive and repulsive cues (reviewed in Mogilner et al., 2003), in addition to environmental factors. Analyzing both the response to attractive signals, as in individual space, and to repulsive signals, as in social avoidance, can help differentiate between different kinds of social deficits. Individuals who do not perform well in either assay would not recognize or care for social signals, and could be characterized as socially indifferent. However, individuals who would have a bigger individual space, but strong avoidance of stressed individuals would be efficient at recognizing social signals, and decide to avoid interactions; thus could be characterized as socially avoidant. We found that despite proper olfaction (data not shown), *rg* mutants unlike the CS control, tend to not avoid the stress odorant left by stressed flies. Instead, they settle further away from their neighbors. It is worth noting that the speed of flies in motion or their activity levels does not affect the distance at which flies choose to finally settle when they form immobile groups (data not shown). Thus, our behavior data suggest that *rg* mutant flies are socially indifferent, since they are less responsive both to stressful social signals in the avoidance assay, and to their neighbor in a stable group.

Our findings on several aspects of synaptic properties, from formation and development of synaptic structures, to synaptic release, and postsynaptic response amplitude, and behavioral output, suggest a functional role for Rugose at the synapse. These results are consistent with the working hypothesis that *rg* is important for targeting and/or sequestering various proteins of cAMP-PKA signaling pathways to specific areas in the neuron. In addition to this potential role at the synapse, we found that Rugose functions in pathways involved in regulating behavior, both at the larval and adult stages, to modulate locomotion, activity levels and response to social signals. The high degree of structural and functional similarity between *rg* and *NBEA* suggests an evolutionarily conserved functional role essential for synapse formation and transmission, in pathways of conserved function, making *rugose* a good candidate gene for studies on autism.

Acknowledgments

We thank Dr. Wes Gruber (Columbia University) for the generous use of his larval tracking equipment. We are grateful to Dr. Sally Hoskins (CCNY) for comments and suggestions on the manuscript. Research presented here was supported by grants from the NIH (T.V and C-F. W). A.W. was supported by NIH-RISE and LSAMP grants at the City College. A.F.S. was supported by PSC-CUNY Awards, jointly funded by The Professional Staff Congress, and, the City University of New York and by internal funding from Western University, Ontario, Canada. R.W.F. was supported by a scholarship from The Alliance/Merck Ciencia Hispanic Scholars Program for STEM College students. The work at City College was supported by NIH-RCMI grant # 8G12MD007603-29.

References

Abrahams BS, Geschwind DH. Advances in autism genetics: on the threshold of a new neurobiology. Nat Rev Genet. 2008; 9(5):341–355.10.1038/nrg2346 [PubMed: 18414403]

Banerjee S, Riordan M, Bhat MA. Genetic aspects of autism spectrum disorders: insights from animal models. Front Cell Neurosci. 2014; 8:58.10.3389/fncel.2014.00058 [PubMed: 24605088]

Berry-Kravis E, Ciurlionis R. Overexpression of fragile X gene (FMR-1) transcripts increases cAMP production in neural cells. J Neurosci Res. 1998; 51(1):41–48. [PubMed: 9452307]

Broadie K, Bate M. Activity-dependent development of the neuromuscular synapse during Drosophila embryogenesis. Neuron. 1993; 11(4):607–619. [PubMed: 7691105]

Budnik V, Zhong Y, Wu CF. Morphological plasticity of motor axons in Drosophila mutants with altered excitability. J Neurosci. 1990; 10(11):3754–3768. [PubMed: 1700086]

Burg ED, Langan ST, Nash HA. Drosophila Social Clustering is Disrupted by Anesthetics and in narrow abdomen Ion Channel Mutants. Genes, Brain and Behavior. 2013 In Press. 10.1111/gbb.12025

Castermans D, Wilquet V, Parthoens E, Huysmans C, Steyaert J, Swinnen L, et al. The neurobeachin gene is disrupted by a translocation in a patient with idiopathic autism. J Med Genet. 2003; 40(5):352–356. [PubMed: 12746398]

Dell'Acqua ML, Smith KE, Gorski JA, Horne EA, Gibson ES, Gomez LL. Regulation of neuronal PKA signaling through AKAP targeting dynamics. Eur J Cell Biol. 2006; 85(7):627–633.10.1016/j.ejcb.2006.01.010 [PubMed: 16504338]

Engel JE, Wu CF. Interactions of membrane excitability mutations affecting potassium and sodium currents in the flight and giant fiber escape systems of Drosophila. J Comp Physiol A. 1992; 171(1):93–104. [PubMed: 1328625]

Engel JE, Wu CF. Altered habituation of an identified escape circuit in Drosophila memory mutants. J Neurosci. 1996; 16(10):3486–3499. [PubMed: 8627381]

Engel JE, Wu CF. Genetic dissection of functional contributions of specific potassium channel subunits in habituation of an escape circuit in *Drosophila*. J Neurosci. 1998; 18:2254–2267. [PubMed: 9482810]

Feng Y, Ueda A, Wu CF. A modified minimal hemolymph-like solution, HL3.1, for physiological recordings at the neuromuscular junctions of normal and mutant Drosophila larvae. J Neurogenet. 2004; 18(2):377–402.10.1080/01677060490894522 [PubMed: 15763995]

Fernandez RW, Nurilov M, Feliciano O, McDonald IS, Simon AF. Straightforward Assay for Quantification of Social Avoidance in Drosophila melanogaster. J Vis Exp. 2014;(94)10.3791/52011

Geschwind DH. Advances in autism. Annu Rev Med. 2009; 60:367–380.10.1146/annurev.med.60.053107.121225 [PubMed: 19630577]

Han JD, Baker NE, Rubin CS. Molecular characterization of a novel A kinase anchor protein from Drosophila melanogaster. J Biol Chem. 1997; 272(42):26611–26619. [PubMed: 9334242]

Jan YN, Jan LY, Dennis MJ. Two mutations of synaptic transmission in Drosophila. Proc R Soc Lond B Biol Sci. 1977; 198(1130):87–108. [PubMed: 20636]

Keshishian H, Kim YS. Orchestrating development and function: retrograde BMP signaling in the Drosophila nervous system. Trends Neurosci. 2004; 27(3):143–147.10.1016/j.tins.2004.01.004 [PubMed: 15036879]

Kidokoro Y, Nishikawa K. Miniature endplate currents at the newly formed neuromuscular junction in Drosophila embryos and larvae. Neurosci Res. 1994; 19(2):143–154. [PubMed: 8008242]

Kuromi H, Ueno K, Kidokoro Y. Two types of Ca2+ channel linked to two endocytic pathways coordinately maintain synaptic transmission at the Drosophila synapse. Eur J Neurosci. 2010; 32(3):335–346.10.1111/j.1460-9568.2010.07300.x [PubMed: 20704589]

Levin LR, Han PL, Hwang PM, Feinstein PG, Davis RL, Reed RR. The Drosophila learning and memory gene rutabaga encodes a Ca2+/Calmodulin-responsive adenylyl cyclase. Cell. 1992; 68(3):479–489. [PubMed: 1739965]

Medrihan L, Rohlmann A, Fairless R, Andrae J, Doring M, Missler M, et al. Neurobeachin, a protein implicated in membrane protein traffic and autism, is required for the formation and functioning of central synapses. J Physiol. 2009; 587(Pt 21):5095–5106.10.1113/jphysiol.2009.178236 [PubMed: 19723784]

Michel JJ, Scott JD. AKAP mediated signal transduction. Annu Rev Pharmacol Toxicol. 2002; 42:235–257.10.1146/annurev.pharmtox.42.083101.135801 [PubMed: 11807172]

Mogilner A, Edelstein-Keshet L, Bent L, Spiros A. Mutual interactions, potentials, and individual distance in a social aggregation. J Math Biol. 2003; 47(4):353–389. Epub 2003 May 2015. [PubMed: 14523578]

Nagai R, Hashimoto R, Yamaguchi M. Drosophila Syntrophins are involved in locomotion and regulation of synaptic morphology. Exp Cell Res. 2010; 316(14):2313–2321. [PubMed: 20632467]

Nair R, Lauks J, Jung S, Cooke NE, de Wit H, Brose N, et al. Neurobeachin regulates neurotransmitter receptor trafficking to synapses. J Cell Biol. 2013; 200(1):61–80.10.1083/jcb.201207113 [PubMed: 23277425]

Niesmann K, Breuer D, Brockhaus J, Born G, Wolff I, Reissner C, et al. Dendritic spine formation and synaptic function require neurobeachin. Nat Commun. 2011; 2:557.10.1038/ncomms1565 [PubMed: 22109531]

Nuytens K, Tuand K, Di Michele M, Boonen K, Waelkens E, Freson K, Creemers JW. Platelets of mice heterozygous for neurobeachin, a candidate gene for autism spectrum disorder, display protein changes related to aberrant protein kinase A activity. Mol Autism. 2013; 4(1): 43.10.1186/2040-2392-4-43 [PubMed: 24188528]

O'Neal J, Gao F, Hassan A, Monahan R, Barrios S, Kilimann MW, et al. Neurobeachin (NBEA) is a target of recurrent interstitial deletions at 13q13 in patients with MGUS and multiple myeloma. Exp Hematol. 2009; 37(2):234–244.10.1016/j.exphem.2008.10.014 [PubMed: 19135901]

Ramaswami M, Krishnan KS, Kelly RB. Intermediates in synaptic vesicle recycling revealed by optical imaging of Drosophila neuromuscular junctions. Neuron. 1994; 13(2):363–375. [PubMed: 8060617]

Rizo J, Sudhof TC. Snares and Munc18 in synaptic vesicle fusion. Nat Rev Neurosci. 2002; 3(8):641–653.10.1038/nrn898 [PubMed: 12154365]

Savelyeva L, Sagulenko E, Schmitt JG, Schwab M. The neurobeachin gene spans the common fragile site FRA13A. Hum Genet. 2006; 118(5):551–558.10.1007/s00439-005-0083-z [PubMed: 16244873]

Shamloula HK, Mbogho MP, Pimentel AC, Chrzanowska-Lightowlers ZM, Hyatt V, Okano H, Venkatesh TR. rugose (rg), a Drosophila A kinase anchor protein, is required for retinal pattern formation and interacts genetically with multiple signaling pathways. Genetics. 2002; 161(2):693–710. [PubMed: 12072466]

Sigrist SJ, Reiff DF, Thiel PR, Steinert JR, Schuster CM. Experience-dependent strengthening of Drosophila neuromuscular junctions. J Neurosci. 2003; 23(16):6546–6556. [PubMed: 12878696]

Simon AF, Chou MT, Salazar ED, Nicholson T, Saini N, Metchev S, et al. A simple assay to study social behavior in Drosophila: measurement of social space within a group. Genes, Brain and Behavior. 2012; 11(2):243–252.10.1111/j.1601-183X.2011.00740.x

Song W, Ranjan R, Dawson-Scully K, Bronk P, Marin L, Seroude L, et al. Presynaptic regulation of neurotransmission in Drosophila by the g protein-coupled receptor methuselah. Neuron. 2002; 36(1):105–119. [PubMed: 12367510]

Stewart BA, Atwood HL, Renger JJ, Wang J, Wu CF. Improved stability of Drosophila larval neuromuscular preparations in haemolymph-like physiological solutions. J Comp Physiol A. 1994; 175(2):179–191. [PubMed: 8071894]

Suh GSB, Wong AM, Hergarden AC, Wang JW, Simon AF, Benzer S, et al. A single population of olfactory sensory neurons mediates an innate avoidance behaviour in Drosophila. Nature. 2004; 431(7010):854–859. [PubMed: 15372051]

Thomas JB, Wyman RJ. Mutations altering synaptic connectivity between identified neurons in Drosophila. J Neurosci. 1984; 4(2):530–538. [PubMed: 6699687]

Ueda A, Wu CF. Role of rut adenylyl cyclase in the ensemble regulation of presynaptic terminal excitability: reduced synaptic strength and precision in a Drosophila memory mutant. J Neurogenet. 2009; 23(1–2):185–199.10.1080/01677060802471726 [PubMed: 19101836]

Volders K, Nuytens K, Creemers JW. The autism candidate gene Neurobeachin encodes a scaffolding protein implicated in membrane trafficking and signaling. Curr Mol Med. 2011; 11(3):204–217. [PubMed: 21375492]

Volders K, Scholz S, Slabbaert JR, Nagel AC, Verstreken P, Creemers JW, et al. Drosophila rugose is a functional homolog of mammalian Neurobeachin and affects synaptic architecture, brain morphology, and associative learning. J Neurosci. 2012; 32(43):15193–15204.10.1523/JNEUROSCI.6424-11.2012 [PubMed: 23100440]

Wu CF, Ganetzky B, Jan LY, Jan YN, Benzer S. A Drosophila mutant with a temperature-sensitive block in nerve conduction. Proc Natl Acad Sci U S A. 1978; 75(8):4047–4051. [PubMed: 211514]

Zhao J, Lu Y, Zhao X, Yao X, Shuai Y, Huang C, et al. Dissociation of rugose-dependent short-term memory component from memory consolidation in Drosophila. Genes Brain Behav. 2013; 12(6):626–632.10.1111/gbb.12056 [PubMed: 23790035]

Zhong Y, Wu CF. Alteration of four identified K+ currents in Drosophila muscle by mutations in eag. Science. 1991a; 252(5012):1562–1564. [PubMed: 2047864]

Zhong Y, Wu CF. Altered synaptic plasticity in Drosophila memory mutants with a defective cyclic AMP cascade. Science. 1991b; 251(4990):198–201. [PubMed: 1670967]

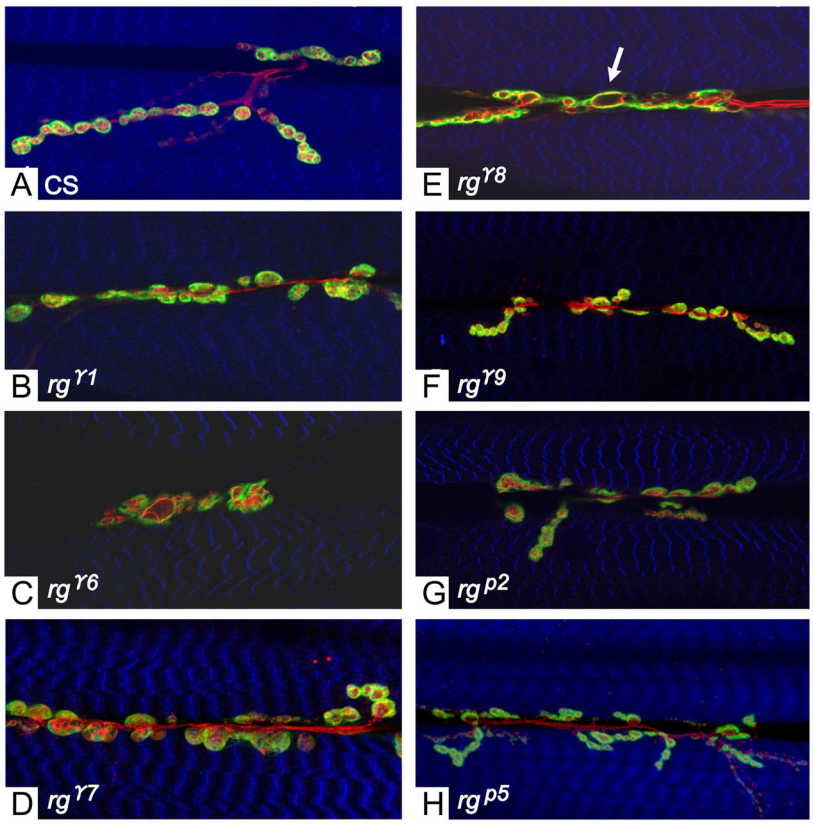

Figure 1. *rg* mutants exhibit altered synaptic structure

Confocal images of the neuromuscular junction from third-instar larvae stained with antibodies: anti-Dlg (green) anti-HRP (red) and Phalloidin (blue). (A) Canton-S. (B–H) In *rg* mutant alleles, bouton numbers are decreased and boutons are slightly enlarged. (E) Few axonal branching and vacuous spacing in the boutons are seen (arrow). *rg* mutant alleles rg^{p2} (G) and rg^{p5} (H) exhibit less severe phenotype than the other gamma alleles. All images (A–H) are from Muscles 6 and 7 in segment 3.

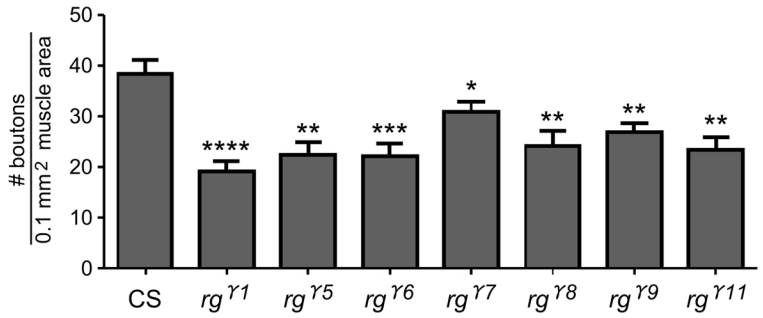

Figure 2. *rg* mutants show aberrant synaptic bouton distribution

The numbers of type I boutons were determined following staining with Anti-Discs large (dlg) and anti-Horseradish peroxidase (HRP) antibodies. Dlg and HRP positive boutons were counted from muscles 6 and 7 in segments A2 and A3. Counts were analyzed by ACT-1 software (Nikon Digital Eclipse DXM 1200) and p values were determined by Student's two-tailed t-test (Prism). When compared to CS, significant decreases in type-I bouton number were observed in the following alleles : $rg^{\gamma 1}$, $rg^{\gamma 5}$, $rg^{\gamma 6}$, $rg^{\gamma 7}$, $rg^{\gamma 8}$, $rg^{\gamma 9}$, $rg^{\gamma 11}$ ($rg^{\gamma 9}$, $p<0.0001^{****}$, n=10; $rg^{\gamma 1}$, $p<0.0001^{****}$, n=10; $rg^{\gamma 6}$, $p<0.001^{***}$, n=11; $rg^{\gamma 5}$, $p<0.01^{**}$, n=8; $rg^{\gamma 8}$, $p<0.01^{**}$, n=11; $rg^{\gamma 11}$, $p<0.01^{**}$, n=7; $rg^{\gamma 7}$, $p<0.05^{*}$, n=15).

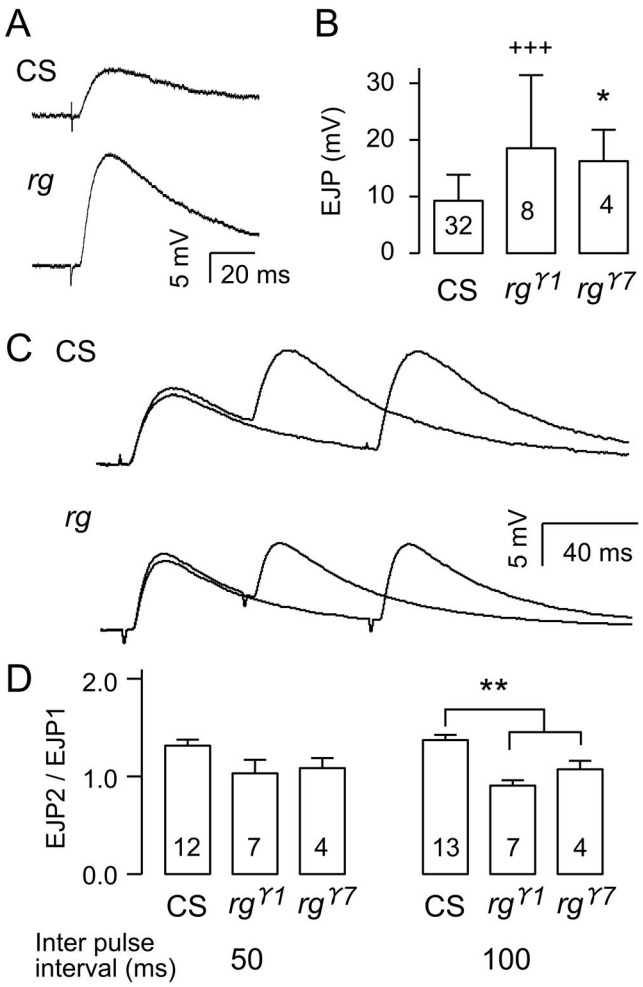

Figure 3. Abnormal synaptic transmission in *rg* larval NMJs

(A) Examples of EJP recordings from wild type and *rg* mutants following nerve stimulation. B) EJP amplitudes in CS and *rg* mutants. +++ indicates $p < 0.001$ (F-test), n=32 (CS), * indicates $p < 0.05$ (t-test), n=8 (rg^{r1}) and *n=4* (rg^{r7}). Both tests were carried out with sequential Bonferroni correction for two *rg* alleles against CS. *rg* mutants exhibit decreased paired pulse facilitation. (C) Sample traces comparing paired pulse facilitation in *rg* and CS. The EJP traces of 50 and 100 ms inter-pulse intervals were overlaid for both CS and *rg*. Each trace is from the average of 7–8 trials. (D) Paired pulse facilitation values in CS and *rg* mutants. ** indicates $p < 0.01$ for both rg^{r1} and rg^{r7} (One way ANOVA). Error bars indicate SEM. Numbers inside the bar graphs indicate the number of NMJs recorded from CS and *rg* mutants.

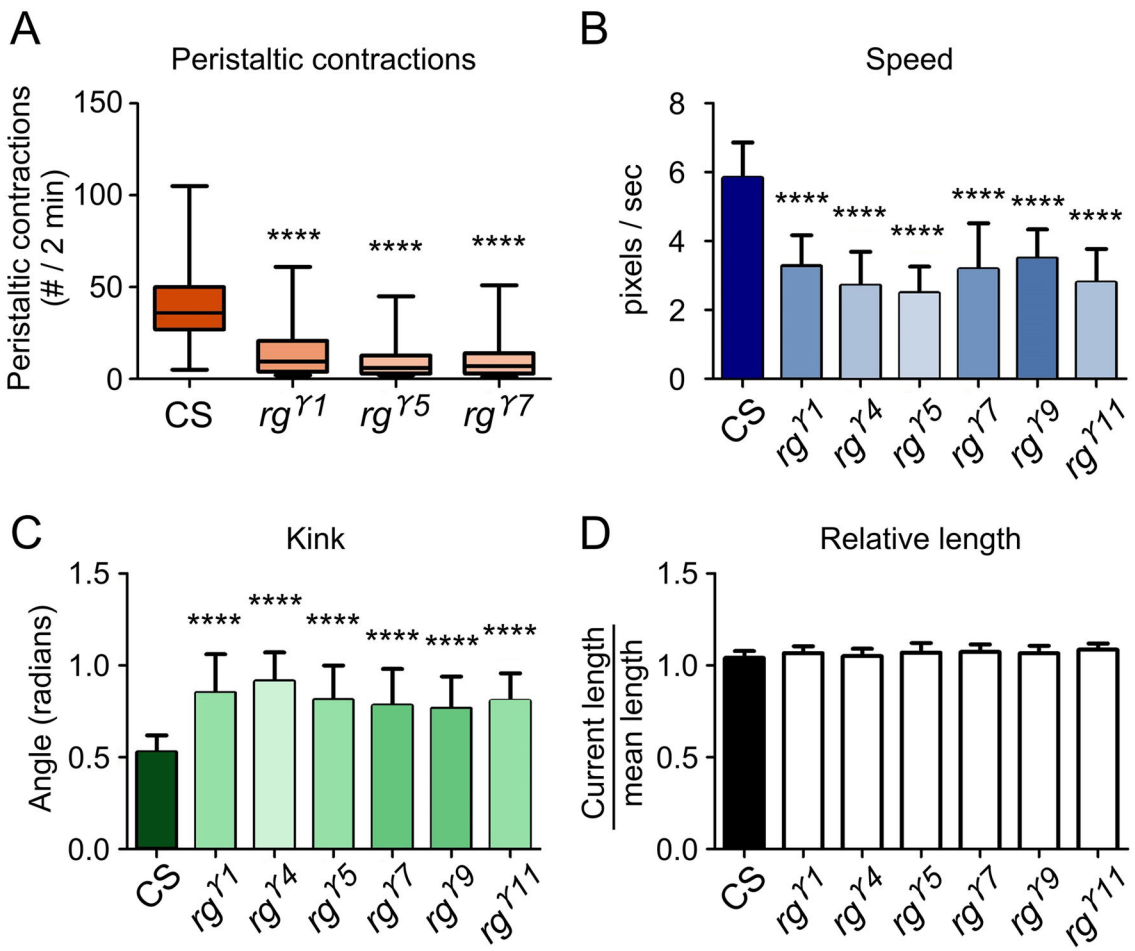

Figure 4. *rg* mutant larvae show aberrant locomotion

(A) Shows larval peristaltic contraction frequencies in CS (n=100) and *rg* mutants. $rg^{\gamma 7}$ (n= 100, p<0.0001), $rg^{\gamma 5}$ (n= 100, p<0.0001) and $rg^{\gamma 1}$ (n=100, p<0.0001). (B) Larval locomotion velocity data from "Worm Tracker" experiments. *rg* mutants have a slower velocity than CS. $rg^{\gamma 1}$ (n= 102, p<0.0001), $rg^{\gamma}{}_{4}$ (n=100, p<0.0001), $rg^{\gamma 5}$ (n=103, p<0.0001), $rg^{\gamma 7}$ (n=100, p<0.0001) and $rg^{\gamma 9}$ (n=103, p<0.0001). (C) Measurements of "kink" or the degree of larval body coiling in *rg* mutants compared to CS. $rg^{\gamma 1}$ (n= 102, p<0.0001), $rg^{\gamma 4}$ (n=100, p<), $rg^{\gamma 5}$ (n=103, p<0.0001), $rg^{\gamma 7}$ (n=100, p<0.0001), $rg^{\gamma}{}_{9}$ (n=103, p<0.0001) and $rg^{\gamma 11}$ (n=102, p<0.0001). (D) Relative larval length measurements fromCS and *rg* mutants.

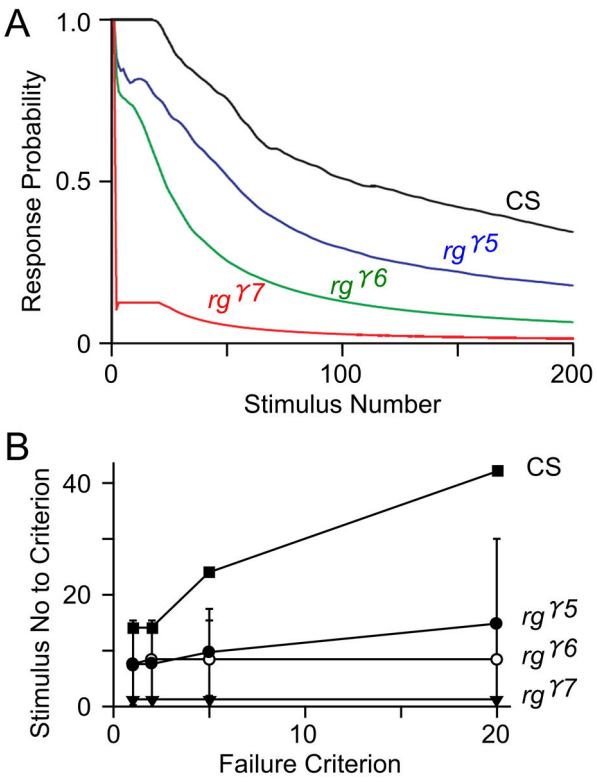

Figure 5. Increased habituation rates of the giant fiber-mediated jump-and-flight escape reflex in adult *rg* mutants

(A) Kinetics of habituation as determined by response probability to 5-Hz brain stimulation. Decline in response probability over time in $rg^{\gamma 5}$, $rg^{\gamma 6}$ and $rg^{\gamma 7}$ mutants are compared to CS. (B) The number of 5-Hz stimuli required to attain criteria of 1, 2, 5, or 20 consecutive failures for different genotypes. The *rg* mutants showed clear differences from CS with a criterion of 5 consecutive failures. The increased habituation rate became even more evident if a criterion of 20 consecutive failures was applied.

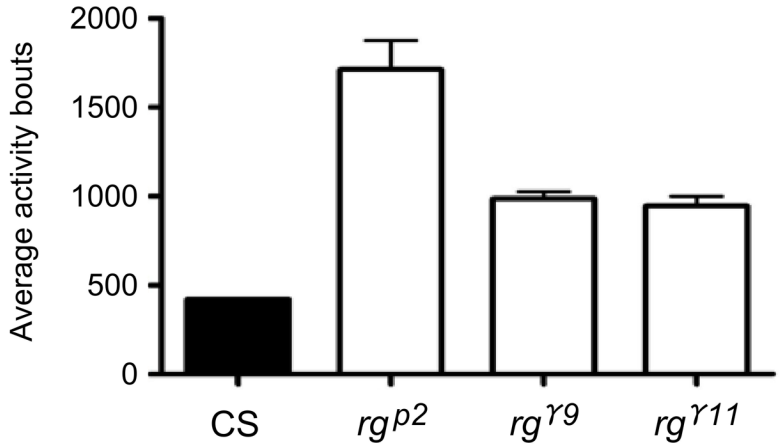

Figure 6. Hyperactivity in *rg* adults: Quantification of average bouts

rg adult mutants are significantly more active than wild type. Adult CS flies displayed a daily average of 421 activity bouts (beam crossings) over four days. $rg^{\gamma 11}$, $rg^{\gamma 9}$ and rg^{P2} showed daily averages of 945, 986, 1712 activity bouts, and thus a 220–400% increase in activity compared to CS ($p<.0001$. ANOVA).

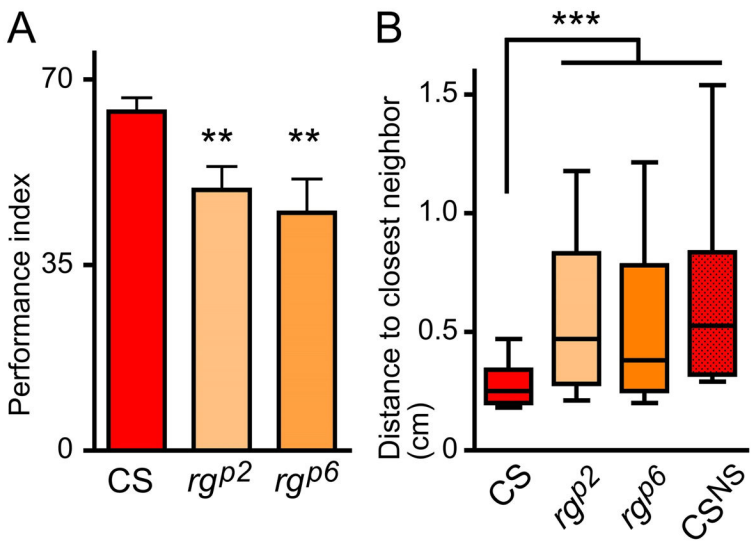

Figure 7. *rg* mutations cause disruptions in adult social behavior

(A) *rg* mutants do not avoid dSO. Bar graph represents the average ± SEM of the Performance Index (PI) of avoidance of the stress odor left by agitated flies; n=5 independent trials of 2 to 3 internal replicates with 40 flies each ($p<0.03$, ANOVA, compared to CS $p<0.01$**). (B) *rg* mutants are indifferent to other flies in a social group ($p<0.0001$, Kruskal-Wallis). Box and whiskers graphs represent the distribution of distance to the closest neighbor in cm, with Turkey's whiskers; data represent three independent experiments with two to three internal replicates of 40 flies. More than 50% of CS flies stayed between 0–0.25 cm away from their closest neighbor, or within around one body length of each other (three independent replicates of two to three internal replicates of 40 flies, n= 240 flies). rg^{p2} (n= 280 flies) and rg^{p6} (n= 320 flies) exhibited less social interaction, preferring to be further apart overall. Their distribution is not different from that of CS^{NS} obtained when analyzing a merged image of 40 single flies ("CS, No Social interactions"), suggesting that the flies' distribution is independent of the presence of other individuals.